Some aspects of flow control over a NACA0015 airfoil using synthetic jets

T Parthasarathy* and S P Das

Department of Mechanical Engineering, Indian Institute of Technology Madras, Chennai 600036, India

E-mail: * tejaswin.sarathy@gmail.com

Abstract. Flow control for performance enhancement over airfoils has become an increasingly important topic. This work details the characteristics of flow control using synthetic jets over a NACA0015 airfoil at a Reynolds number of 896,000 based on the chord length and free stream velocity, and at 20° angle of attack wherein the flow is separated. Numerical simulations were performed to help understand the behaviour of the controlled flow for a range of synthetic jet parameters. Analysis of key flow parameters such as phase averaged pressure and streamline profiles indicate that the synthetic jet is efficient in increasing the lift coefficient; more so for larger jet amplitudes and at smaller angles of jet injection. Behaviour of the flow characteristics for controlled cases has been analysed from the flow structures obtained from the same. This work serves as a platform to qualitatively and quantitatively understand the effects of the jet parameters on the separated flow over the airfoil.

1. Introduction

Unsteady active flow control has been an actively pursued area of research in the past decades. A major advantage of such an unsteady control technique is that it can exploit the existing instabilities in the flow [1]. Periodic excitation accelerates and regulates the generation of large coherent structures with the flow and hence transfers high momentum fluid across the mixing layer. Of particular interest in periodic excitation control is the use of zero net mass flux devices, also called synthetic jets [2]. Synthetic jets are formed by oscillatory flow through an orifice. Hence, while similar to continuous jets (used for suction and blowing) in form and function, they vary in the fact that they offer no mass addition (or removal), entrain low momentum fluid [3] and promote mixing through the formation of vortical structures. The performance of the synthetic jets in controlling a flow greatly relies on the amplitude, frequency, inclination angle and location of the synthetic jets [4,5,6].

Several experimental and numerical works in characterizing the flow control over an airfoil have been done in the past. Experimental data for the same airfoil at different angles of attack for a Reynolds number ($Re = UCv^{-1}$, where U is the free stream velocity, C is the chord length and v is the kinematic viscosity) of 896,000 [7] suggests that the maximum lift coefficient value can be enhanced by 80% and the stall angle can be pushed back from 12° to 18°. The effectiveness of using synthetic jets for stall control over airfoils was also demonstrated experimentally [8,9]. Numerical studies also demonstrate and characterize the effect of synthetic jets on a wide range of airfoils at different angles of attack [10,11,12]. Duvigneau and Visonneau [13] explore the effect of jet parameters on the lift and

drag coefficients for a NACA0015 airfoil at the same Reynolds number, and suggest an increase in the lift by 34%.

In the present study, numerical investigations have been carried out to understand the effects of the synthetic jet and its parameters on the external flow over a NACA0015 airfoil at an angle of attack of 20° for a Reynolds number of 896,000, based on the free stream velocity and chord. Thrust is also given in understanding the reason behind the performance enhancement on using the synthetic jets in such separated flows. The jet location and width are fixed based on previous studies [12,14]. The important jet parameters chosen are summarised in table 1.

Table 1. Summary of parameters

Non dimensional Frequency ($F = fC\,U^{-1}$)	Amplitude Ratio at jet exit ($VR = V_j\,U^{-1}$)	Angle of jet injection (in °)
0.6446	1.50	30
0.9670	2.00	45
1.1281	2.25	60
1.2893	2.50	90
1.6117	3.00	-

2. Basic Flow

An external flow over an airfoil has been studied, with suitable modifications to include the model of a synthetic jet. The equations to be solved are the incompressible two-dimensional continuity and Navier Stokes equations, elaborated as follows (where $\vec{V}$, P, ρ and μ are velocity, pressure, density and dynamic viscosity respectively)

$$\nabla.\vec{V}=0 \tag{1}$$

$$\frac{d\vec{V}}{dt}+(\vec{V}.\nabla)\vec{V}=-\frac{1}{\rho}\nabla P+\frac{\mu}{\rho}\nabla^2\vec{V} \tag{2}$$

3. Case Setup

3.1. Geometrical setup and Boundary conditions

The geometrical setup and corresponding boundary conditions are as shown in figure 1. An inlet velocity of 34.9 ms^{-1} is specified, corresponding to a Reynolds number of 896,000 for air, with very low turbulent intensity. The chord length is taken as 0.375m, with a single slot of width $0.0053C$ at $0.12C$ from the leading edge. Other geometrical details are avoided for the sake of brevity. The steady flow Neumann boundary condition is imposed at the exit. The airfoil wall is given a no-slip boundary condition. A time varying sinusoidal boundary condition is given at the sinusoidal velocity inlet shown (figure 1) in such a way that at the jet exit, the flow is fully developed and has an exit velocity of V_j .

$$V_i=VR\times U\times \sin(2\pi ft) \tag{3}$$

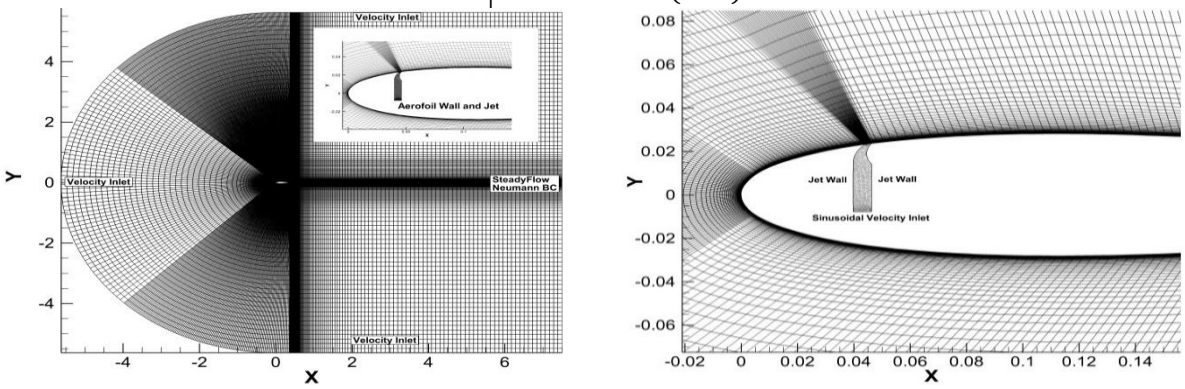

Figure 1. Representative mesh with geometry & boundary conditions, for an injection angle of 30°

3.2. Numerical Scheme

The simulations were set up in the commercial CFD solver Fluent, at 20° angle of attack. This particular configuration is studied as the baseline flow is completely separated, and hence the effect of the jet will be predominant. The velocity at the base of the jet is taken such that the average velocity at the jet exit is VR × U. A time implicit second order upwind discretization scheme with the SIMPLE coupling, was used to solve the equations that were derived based on the Spalart-Allmaras model. The simulations were run till a quasi (dynamic)- steady state is reached for the system.

3.3. Grid Setup

Different meshes were generated for different angles of injection, and the details of the mesh also change. A grid independence test was done for all the aforesaid grids, with cells numbering 35,200, 74,879 and 144,000. Based on the same, the mesh with 74,879 cells is selected. The spacing values ($\Delta c/C$) near the jet exit is 2.01×10^{-4}, at the point of maximum near the airfoil wall is 7.36×10^{-3} and normal to the wall is 2.6×10^{-5}(corresponding to a y^+ value of 1). The grid size for the semi-circular inlet, horizontal and vertical edges is 363×120×240.

3.4. Validation

The validation of the current setup is done by comparing the obtained values with the results of [13] and XFoil data as shown in figure 2 (experimental validation is avoided due to reasons stated in [13]), which suggests a reasonable match. The same can be said for the streamlines in the uncontrolled flow.

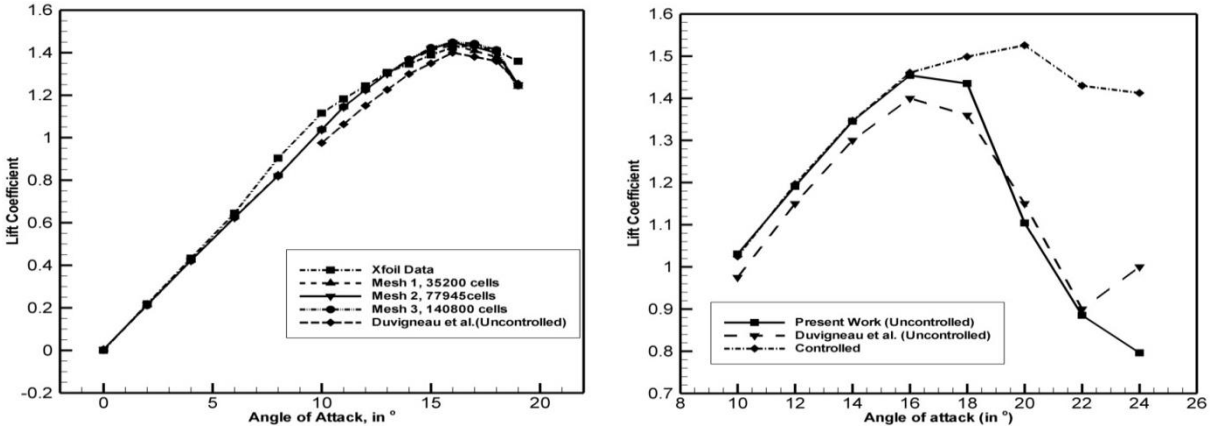

Figure 2. Validation of lift coefficient data, from data through Xfoil and Duvigneau et al. [13]

4. Results and Discussions

4.1. Effect of jet parameters

Extensive simulations were performed to identify the effect of the parameters on the external flow. The lift characteristics were observed for all the cases. The effects of the parameters on the flow become apparent on analysing the same, many of which are avoided here for the sake of brevity.

The slope of the lift coefficient graph (figure 3 (a)) with injection angle changes abruptly, except for the case of 150 Hz frequency, wherein it decreases linearly. The nature of the graph seems to suggest a local maxima and minima at around 45° - 60 ° angles of injection, which becomes less pronounced at higher frequencies. While at lower amplitudes, the lift versus angle curve is concave upwards, this slowly changes to a concave downwards curve at higher amplitudes. However, this effect is barely visible at the highest frequency tested. Lift also increases substantially at lower angles of injection, if other parameters are kept the same.

The lift values in the case of 90° angle of injection do not display any trend with different amplitudes (figure 3(b)), and is also among the least measured values. Lift characteristics plotted against amplitude ratios suggest an upward concave monotonic curve for all angles of attack except at 90°. The graph flattens out as the angle of injection increases. Lift increases substantially at higher

amplitudes, with other parameters kept the same. As amplitude is the most important factor tested, the values of lift/drag are also represented in figure 3(d).

At higher amplitudes and smaller angles, the frequency of operation becomes increasingly irrelevant for lift enhancement, as visible in the figure 3(c). At lower angles and lower amplitudes, the frequency must be kept at a minimum for desirable characteristics. The sensitivity of the lift values to the frequency of operation seems to be minimal at lower angles of injection. However, it is interesting to note that the graph changes concavity from almost zero to concave upwards as the angle increases.

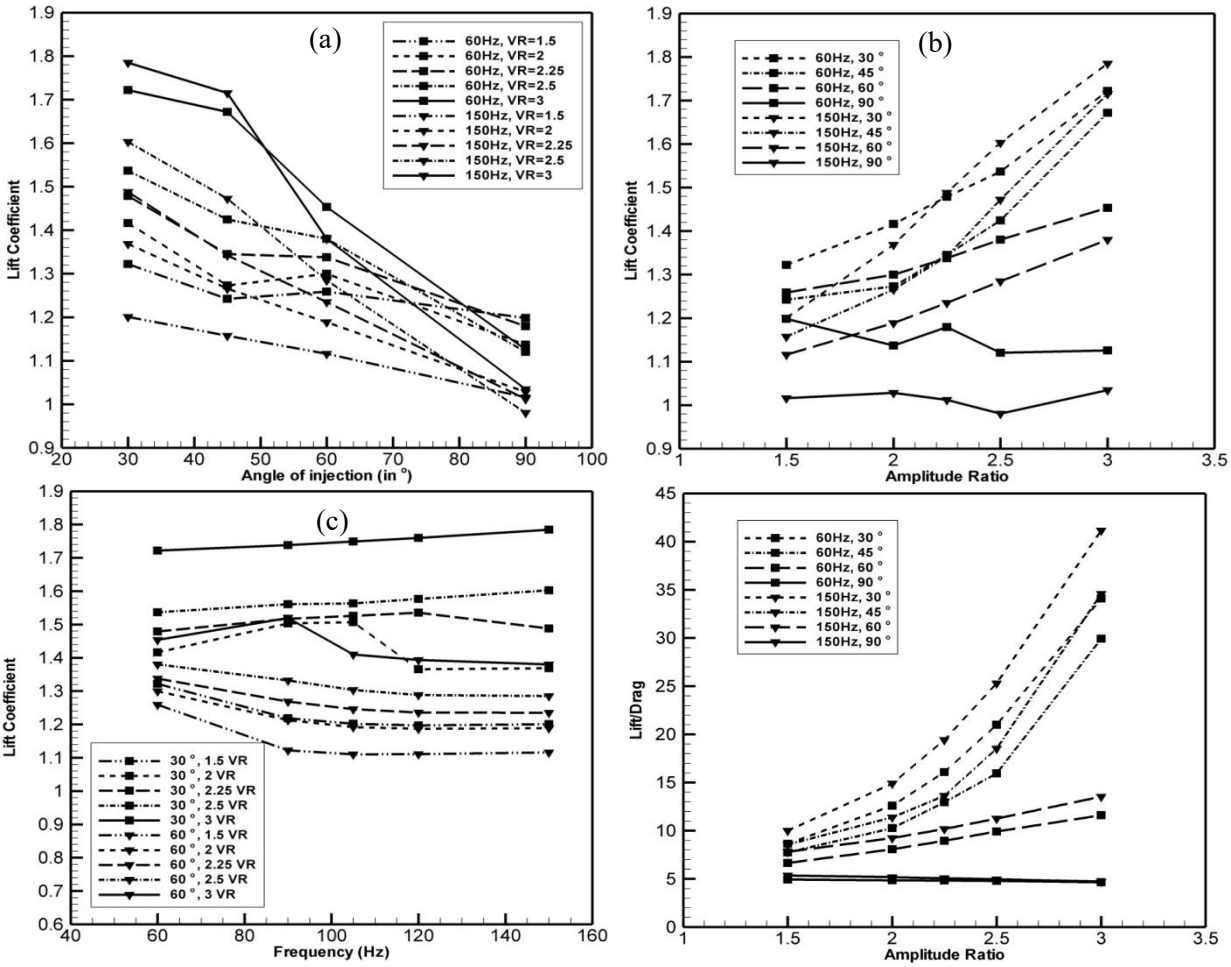

Figure 3. Performance characteristics of the parametric study

4.2. Flow physics

While the previous section details the characteristics and behaviour of the performance of a controlled airfoil with variation in the input parameters, the physics behind the flow is still left unexplained. The controlled flow exhibits different characteristics and flow structures for different frequencies, amplitudes and angles of injection. A comparison to the steady baseline flow at the same angle of attack is also given so as to delineate the cause of increased lift in the controlled cases (figure 4). While the characteristics associated with the change in input parameters are discussed, the detailed flow structure for a representative case is only given.

The controlling aspect of a synthetic jets stems from the fact that it adds momentum flux and vorticity flux to the external flow, without any mass flux addition. The momentum flux is instrumental in separation control, which is done by adding high momentum fluid to the boundary layer during the blowing stroke and by removing the proximal low momentum fluid during the suction stroke, leading to stifled separation. A synthetic jet in a quiescent flow is characterized by the vortex rings (which are

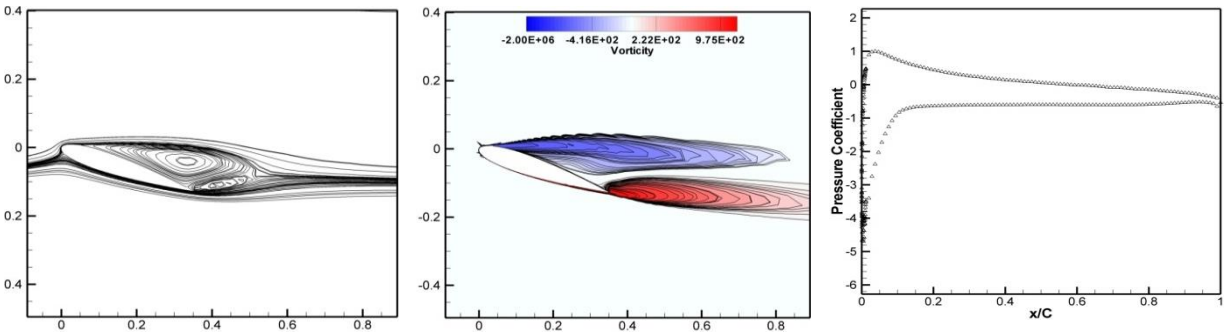

(a) Streamline Contour (b) Vorticity Contour (c) Pressure Distribution

Figure 4. Flow patterns for the baseline(uncontrolled) case

manifested as a pair of counter-rotating vortices in 2D) emanating into the surroundings, which carries the aforesaid momentum, and vorticity flux along with it.

Optimal flow control (using low angles of injection and feasible amplitudes) involves the convective transport of these vortices downstream. Vortices are generated during the blowing stroke, while the suction stroke is marked by coalescence of the external flow. While the strength of the anticlockwise rotating vortex (from the left edge of the synthetic jet wall here) is diminished, the other vortex is sustained and can be seen as a thick blob of vorticity (figure 5). During the suction stroke, the boundary layer seems to have lesser thickness compared to the baseline flow case. While the said vortex is generated due to the jet, its point of manifestation (physical significance) depends on the flow parameters selected. This vortex grows in size during the suction stroke, travelling downstream at the same time (This is seen in both the vorticity and streamline contours of figure 5). This vortex is finally shed (the location of separation depends on the flow parameters) and in case of moderate parameters, present a typical vortex shedding pattern – with an opposite rotating vortex generated

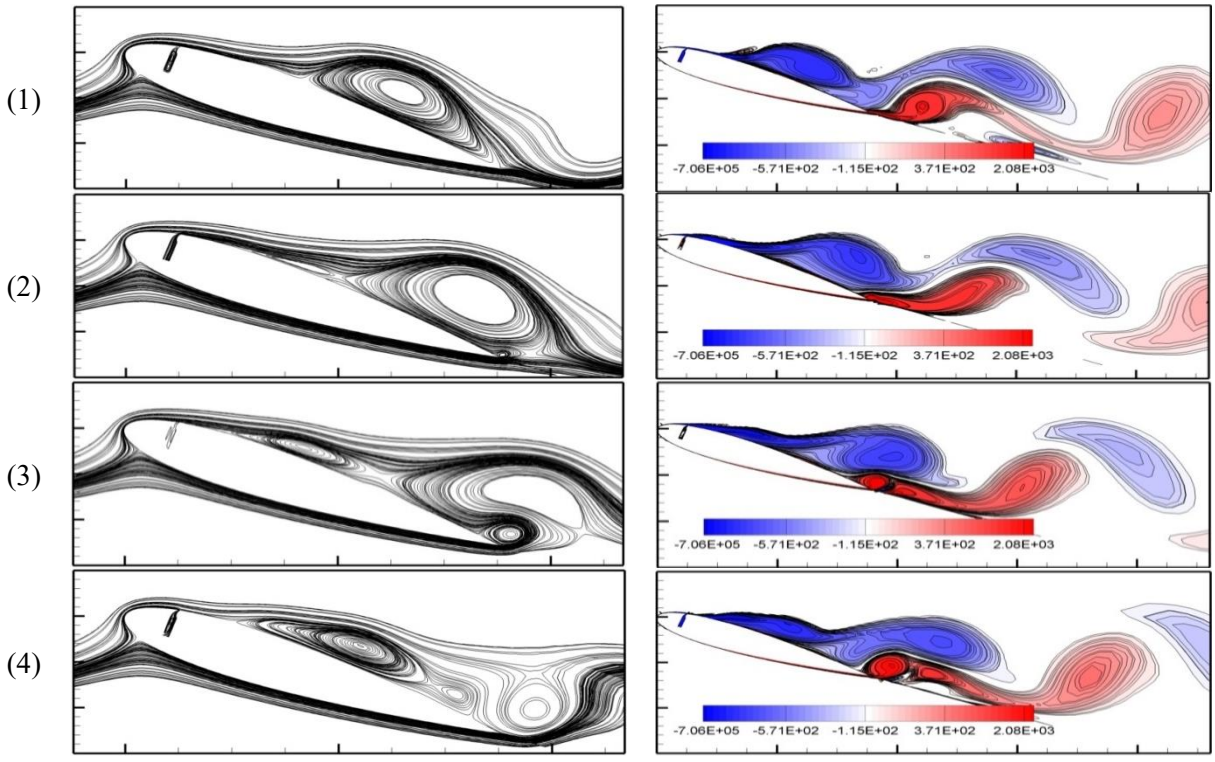

(a) Streamline Contours (b) Vorticity Contours

Figure 5. Phase averaged flow patterns for a controlled case (60Hz, 30^o injection, 1.5 VR) at ϕ = (1) 0^o, (2) 90^o, (3) 180^o, (4) 270^o

from the pressure side of the airfoil. On noticing the phase average pressure coefficient plots, shown in figure 6, it is clearly seen that the vortex emanating from the synthetic jet acts like a low pressure "wave". This wave increases the area bound within the pressure coefficient curve (thus increasing the lift), while at the same time travelling downstream from its point of creation. While this forms the basis for the controlling aspect of the flow, some differences do creep in based on the parameters selected.

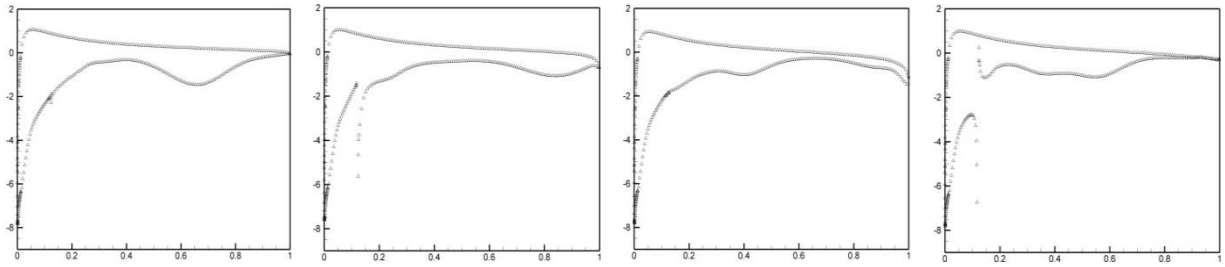

(a) (b) (c) (d)

Figure 6. Phase averaged pressure coefficient distribution for a controlled case (60Hz, 30° injection, 1.5 VR) at ϕ = (1) 0°, (2) 90°, (3) 180°, (4) 270°

Amplitude adversely affects the flow characteristics. With an increase in amplitude, the shed vortices are stretched and continuous (from both the suction side and pressures side of the airfoil). Furthermore, the leading edge separation observed in the baseline case shifts to a trailing edge type separation at higher amplitudes (figure 7). This is attributed to the fact that the vortex formed from the jet does not manifest to significant proportions and is shed almost immediately from the airfoil wall.

Major changes in the flow structures can be witnessed on changing the frequency. For the same amplitudes, vortices appear stretched and continuous at higher frequencies. Changes in the streamline patterns corresponding to the same indicate a constriction of streamlines forming a thinner separation

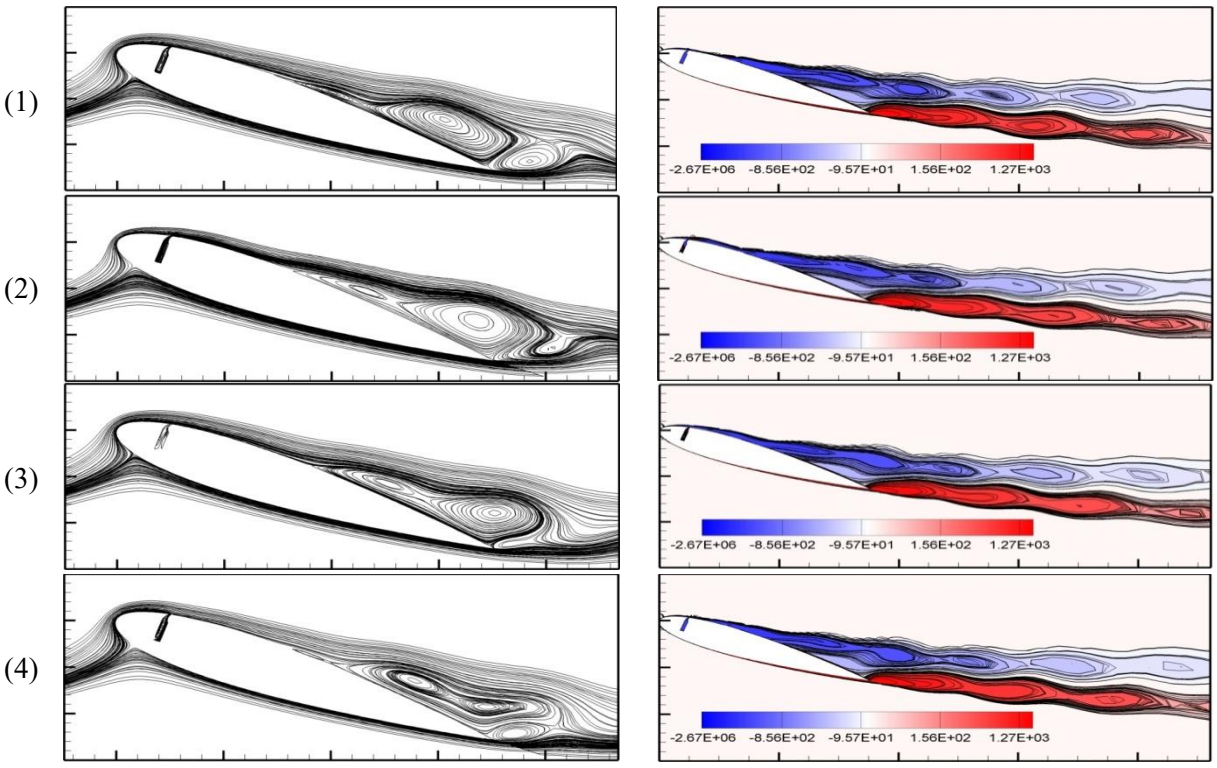

(a) Streamline Contours (b) Vorticity Contours

Figure 7. Phase averaged flow patterns for a controlled case (150Hz, 30° injection, 2.25 VR) at ϕ = (1) 0°, (2) 90°, (3) 180°, (4) 270°

bubble at higher frequencies (figure 7). As the vortices correspond to the frequency of operation, it is understandable that the pressure waves mentioned before correspond to the frequency of operation - more the frequency, more such waves per unit time. However the amplitudes of these waves also decrease, probably owing to the nature of the inherent instabilities in the flow. Cumulatively, a marginal increase in the area under the graph is seen for higher frequencies.

Less surprising is the fact that to maintain optimal control, the angle of injection is to be restricted to a minimal value. With an increase in the angle of injection, the normal component of the velocity increases for the same amplitude. The manifestation of the jet vortex occurs upstream as the angle is increased. As a result, the vortex from the synthetic jet is thus shed earlier from the airfoil, leading to a larger separation region. While the pressure "waves" have higher amplitudes at the jet vortex inception, it quickly diminishes to very low values. A comparison between figure 5 and figure 7 highlights the differences creeping in to the flow structures as the jet parameters are varied.

5. Conclusion

The effect of synthetic jet parameters on the flow control over a NACA0015 airfoil has been studied in depth. Qualitative characteristics for a representative case are given to highlight the effect of the jet on the performance enhancement of the airfoil. Thrust was placed on understanding the physics of the flow and the reason for effective control. Several remarks and explanations were given based on the observed characteristics, paving way for the better understanding of the turbulent physics associated with such jets. While this work serves as a platform to understand the effect of the synthetic jet, several modifications to the same can be made that can better enhance desired characteristics. A study on such parameters will be carried out in the near future.

References

[1] Collis S S, Joslin R D, Seifert A, and Theofilis V 2004 Issues in active flow control: theory, control, simulation, and experiment *Prog. Aerosp. Sci.* **40** 237-89
[2] Glezer A and Amitay M 2002 Synthetic jets *Annu. Rev. Fluid Mech.* **34** 503-29
[3] Smith B L and Swift G W 2003 A comparison between synthetic jets and continuous jets *Exp. Fluids.* **34** 467-72
[4] Mittal R and Rampunggoon P 2002 On the virtual aeroshaping effect of synthetic jets *Phys. Fluids*. **14** 1533-36
[5] Okada K, Fujii K and Miyaji K 2009 Computational study of frequency and amplitude effects on separation flow control with the synthetic jet *Int. Mechanical Engineering Congress and Exposition (Buena Vista)* **9** 289-298
[6] Akcayoz E and Tuncer I H 2009 Numerical Investigation of flow control over an airfoil using synthetic jets and its optimization *Int. Aerospace Conference (Ankara)*
[7] Gilarranz J L, Traub L W and Rediniotis O K 2005 A new class of synthetic jet actuators—part II: application to flow separation control *J. Fluids. Eng.* **127** 377-387
[8] Goodfellow S D, Yarusevych S and Sullivan P E 2009 Momentum coefficient as a parameter for aerodynamic flow control with synthetic jets *AIAA J.* **51** 623-31
[9] Mccormick D C 2000 Boundary layer separation control with directed synthetic jets 38th *Aerospace Sciences Meeting and Exhibit (Reno) AIAA* 519
[10] Raju R, Mittal R and Cattafesta L 2008 Dynamics of airfoil separation control using zero-net mass-flux forcing *AIAA J.* **46** 3103-15
[11] You D and Moin P 2008 Active control of flow separation over an airfoil using synthetic jets *J. Fluid. Struct.* **24** 1349-57
[12] Lasagna D, Donelli S, De Gregorio F, Orazi M and Iuso G 2013 Separation delay on thick airfoil using multiple synthetic jets *XXI Congresso Aimeta (Torino)*
[13] Duvigneau R and Visonneau M 2004 Simulation and optimization of aerodynamic stall control using a synthetic jet *2nd AIAA Flow Control Conf. (Portland)* 2315
[14] Dannenberg RE and Weiberg JA 1952 Section characteristics of a 10.5-percent thick airfoil with area suction as affected by chordwise distribution of permeability *NASA TN 2847*